16th ASCE Engineering Mechanics Conference
July 16-18, 2003, University of Washington, Seattle

EVOLUTION OF STRESS IN DENSE GRANULAR MATERIALS AT THE PEAK STATE OF LOADING

Matthew R. Kuhn [1], Member ASCE

ABSTRACT

When dense granular materials are tested in shear or biaxial compression, the deviatoric stress increases with increasing strain until the deviator stress reaches a peak state. At the peak state, the deviatoric stress is stationary, although the material's volume may be changing. The current study concerns the micro-scale processes that produce a stationary macro-scale stress at the peak state. We consider an unusual decomposition (partition) of the deviatoric stress, in which both changes in the contact forces and in their directions are separately acknowledged. The rate of stress is expressed as a sum of both contributions, and each contribution is further separated into the effects of the tangential and the normal contact forces. We then conduct numerical experiments to quantify each contribution to the average, stationary stress rate at the peak state. The Discrete Element Method is employed in simulations of a large dense assembly of two-dimensional circular disks. The results show that, at the peak state, the average stress is stationary, but that normal contact forces are, on average, increasing. This average increase in the normal forces is offset, in part, by concurrent changes in the tangential forces. The increase in normal force is also offset by changes in the directions of the normal contact forces, since the orientations of the contact normals change when neighboring particle pairs rotate around each other. This unusual result provides further understanding of how stress can evolve in a micro-scale view even as the macro-scale stress is stationary.

Keywords: Granular materials, stress, microstructure, heterogeneous materials

INTRODUCTION

When a dense unbonded granular assembly is loaded in shear or in biaxial or triaxial compression, the deviatoric stress increases with the shear strain until it reaches a peak condition. In loose assemblies, the peak stress is sustained with further loading, but with dense assemblies the peak state is followed by a weakening or softening of the material behavior. The deviatoric stress is, for the moment, stationary at the peak state, although the shear deformation is often accompanied by a volumetric expansion (dilation) of the material. In the paper, we see that a stationary peak stress does not imply a stationary transmission of internal force within the material. Particles continue to be rearranged and the forces among them are continually altered. Although local changes in contact forces might be expected, changes also occur *in the mean*, even as the stress remains constant. The paper explores the mean change in the contact forces at the peak state and offers a rationale for these changes.

---

[1]Dept. of Civil and Env. Engrg., School of Engineering, University of Portland, 5000 N. Willamette, Portland, OR 97203, U.S.A., `kuhn@up.edu`

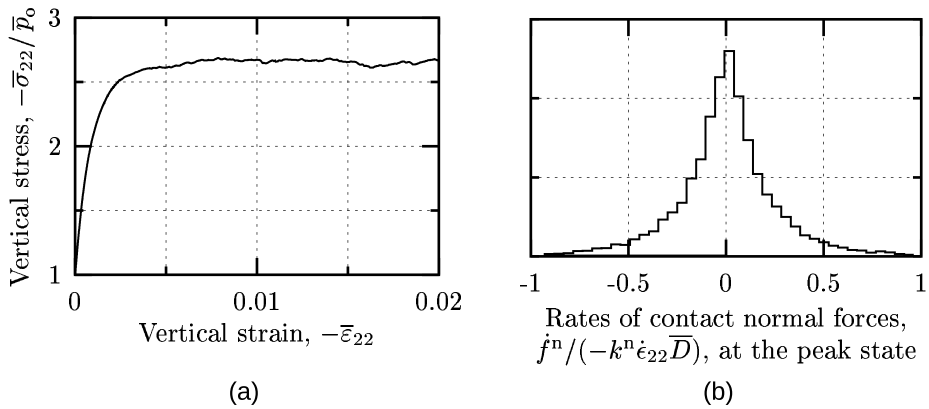

FIG. 1. Results from a numerical DEM simulation of the biaxial compression of 10,816 circular disks: (a) the average stress response, and (b) the changes in the contact normal forces at the peak state.

SIMULATIONS

To investigate the evolution of contact force at the peak state, we have simulated the biaxial compression of a dense, two-dimensional assembly of circular disks. The square assembly contains 10,816 unbonded circular disks of multiple diameters (for details, see Kuhn 2003). The material was compacted from a sparse state, producing a material that was dense, random, and isotropic, at least when viewed at at macro-scale. The average initial void ration was 0.1727 (solid fraction of 0.853), and the average coordination number was 3.82. The initial height and width of the square assembly were each about $102\overline{D}$, where $\overline{D}$ is the mean particle diameter.

A single loading test was conducted. The height of the assembly was reduced at a constant rate of compressive strain ($\dot{\epsilon}_{22} < 0$) while maintaining a constant average horizontal stress along the side boundaries ($\dot{\sigma}_{11} = 0$). During this biaxial compression test, a simple force mechanism was employed between contacting particles. The particles were unbonded, so that no inter-particle tensile forces could develop. The contacts were compliant, with linear normal and tangential springs of equal stiffness ($k^{\rm n} = k^{\rm t}$), and slipping between particles would occur whenever the contact friction coefficient of 0.50 was attained—an inter-particle friction angle of 26.6°.

The material behavior during biaxial compression is shown in Fig. 1a. The assembly reached the peak state at a vertical compressive strain of between 0.0135 and 0.0145, at which the material was dilating rather vigorously at a rate $-(\dot{\epsilon}_{11} + \dot{\epsilon}_{22})/\dot{\epsilon}_{22}$ of about 0.83. Beyond the peak state, the material softened until a steady state condition was attained at a vertical (engineering) strain of about 40%, well beyond the strain in Fig. 1a.

While the average stress was stationary at the peak state, the forces among contacting particles were substantially changing. The extent of these local changes is illustrated in Fig. 1b, a histogram of the rates of change of the normal (compressive) contact forces $f^{\rm n}$ among the over 16,000 contacts at the peak state. The rates in Fig. 1b are expressed in a dimensionless form by dividing by the mean particle diameter $\overline{D}$, the normal contact stiffness $k^{\rm n}$, and the deformation rate $\dot{\epsilon}_{22}$. Because this rate is negative, positive values in the figure imply an increase in (compressive) normal force. The large changes in the normal contact forces are much greater than the average rate $\langle \dot{f}^{\rm n} \rangle$, but this average rate is not zero: contact forces *increase* in the mean, even while the stress is stationary. The dimensionless rate $\langle \dot{f}^{\mathrm{n}} \rangle / (-k^{\mathrm{n}} \dot{\epsilon}_{22} \overline{D})$ is about 0.06 at the peak state.

ANALYSIS

The effect of the increasing normal forces, $\langle \dot{f}^{\mathrm{n}} \rangle$, is counteracted by two other effects, which, together, produce a stationary stress: concurrent changes in the average tangential forces and concurrent changes in the directions of the normal forces. These effects can be investigated through an unusual decomposition of the average stress in a granular material. Details of the decomposition are presented elsewhere, which we now summarize (Kuhn 2003). The average stress $\bar{\boldsymbol{\sigma}}$ in a granular material is computed as

$$\bar{\boldsymbol{\sigma}} = \frac{1}{V} \sum_{pq \in \mathcal{M}} \mathbf{f}^{pq} \otimes \mathbf{l}^{pq} \ , \tag{1}$$

where summation is applied to the set of $\mathcal{M}$ contacts within the assembly, and each contact pq represents an ordered pair of contacting particles p and q (Christoffersen et al. 1981; Rothenburg and Selvadurai 1981). The sum in (1) is of the dyadic products $\mathbf{f}^{pq} \otimes \mathbf{l}^{pq}$, where $\mathbf{f}^{pq}$ is the contact force exerted by particle q upon particle p, and *branch vector* $\mathbf{l}^{pq}$ connects a reference (material) point on particle p to a reference point on particle q. This sum is divided by the bulk assembly volume V.

The separate participation of V, $\mathbf{f}^{pq}$, and $\mathbf{l}^{pq}$ in the stress rate can be investigated with the differential form

$$d\bar{\boldsymbol{\sigma}} = -\frac{dV}{V}\bar{\boldsymbol{\sigma}} + \sum_{pq \in \mathcal{M}} d\mathbf{f}^{pq} \otimes \mathbf{l}^{pq} + \sum_{pq \in \mathcal{M}} \mathbf{f}^{pq} \otimes d\mathbf{l}^{pq} \ , \tag{2}$$

by measuring the small changes dV, $d\mathbf{f}^{pq}$, and $d\mathbf{l}^{pq}$ that occur in a numerical simulation of biaxial compression. Changes in the contact forces $d\mathbf{f}^{pq}$ and in the relative particle positions $d\mathbf{l}^{pq}$ are caused by changes in either the sizes or directions of the vectors $\mathbf{f}^{pq}$ and $\mathbf{l}^{pq}$. We split the vectors $\mathbf{f}^{pq}$ and $\mathbf{l}^{pq}$ into components that are normal and tangent to the contact surfaces, and then we track the changes in the sizes and directions of these components. A contact force $\mathbf{f}^{pq}$ is the sum of its normal and tangential components,

$$\mathbf{f}^{pq} = \mathbf{f}^{pq,\mathrm{n}} + \mathbf{f}^{pq,\mathrm{t}} \ , \tag{3}$$

and each component is the product of a scalar (size) and a unit direction vector,

$$\mathbf{f}^{pq} = f^{pq,\mathrm{n}} \mathbf{n}^{pq} + f^{pq,\mathrm{t}} \mathbf{t}^{pq} \ , \tag{4}$$

where unit vector $\mathbf{n}^{pq}$ is directed outward from particle p and is normal to the contact surface of the pair pq. In an unbonded material, the normal forces $f^{pq,\mathrm{n}}$ are compressive (negative). Because the simulation in this study is two-dimensional, we adopt an unambiguous tangent direction vector $\mathbf{t}^{pq}$—a unit vector directed counterclockwise around particle p.

The force increment $d\mathbf{f}^{pq}$ can be expressed as

$$d\mathbf{f}^{pq} = d f^{pq,\mathrm{n}} \mathbf{n}^{pq} + f^{pq,\mathrm{n}} d\mathbf{n}^{pq} + d f^{pq,\mathrm{t}} \mathbf{t}^{pq} + f^{pq,\mathrm{t}} d\mathbf{t}^{pq} \ , \tag{5}$$

and the incremental change in branch vector $\mathbf{l}^{pq}$ can be expanded in a similar manner:

$$d\mathbf{l}^{pq} = d\ell^{pq,\mathrm{n}} \mathbf{n}^{pq} + \ell^{pq,\mathrm{n}} d\mathbf{n}^{pq} + d\ell^{pq,\mathrm{t}} \mathbf{t}^{pq} + \ell^{pq,\mathrm{t}} d\mathbf{t}^{pq} \ . \tag{6}$$

TABLE 1. Rates of the average Cauchy deviator stress at the peak state

Symbol	Definition[a]	Deviator rate[b, c]
$d\overline{\boldsymbol{\sigma}}^{\text{dv}}$	$-\frac{dV}{V}\overline{\boldsymbol{\sigma}}$	−1.4
$d\overline{\boldsymbol{\sigma}}^{\text{df}^{\text{n}}}$	$\frac{1}{V}\sum d f^{pq,\text{n}} \quad \mathbf{n}^{pq} \otimes \mathbf{l}^{pq}$	14.0
$d\overline{\boldsymbol{\sigma}}^{\text{dn}^{\text{f}}}$	$\frac{1}{V}\sum \quad f^{pq,\text{n}}\, d\mathbf{n}^{pq} \otimes \mathbf{l}^{pq}$	−4.5
$d\overline{\boldsymbol{\sigma}}^{\text{df}^{\text{t}}}$	$\frac{1}{V}\sum d f^{pq,\text{t}} \quad \mathbf{t}^{pq} \otimes \mathbf{l}^{pq}$	−4.1
$d\overline{\boldsymbol{\sigma}}^{\text{dt}^{\text{f}}}$	$\frac{1}{V}\sum \quad f^{pq,\text{t}}\, d\,\mathbf{t}^{pq} \otimes \mathbf{l}^{pq}$	0
$d\overline{\boldsymbol{\sigma}}^{d\ell^{\text{n}};\,\text{f}^{\text{n}}}$	$\frac{1}{V}\sum \quad f^{pq,\text{n}}\, d\ell^{pq,\text{n}}\, \mathbf{n}^{pq} \otimes \mathbf{n}^{pq}$	0
$d\overline{\boldsymbol{\sigma}}^{d\ell^{\text{n}};\,\text{f}^{\text{t}}}$	$\frac{1}{V}\sum \quad f^{pq,\text{t}}\, d\,\ell^{pq,\text{n}}\, \mathbf{t}^{pq} \otimes \mathbf{n}^{pq}$	0
$d\overline{\boldsymbol{\sigma}}^{\text{dn}^{\ell};\,\text{f}^{\text{n}}}$	$\frac{1}{V}\sum \quad f^{pq,\text{n}} \quad \ell^{pq,\text{n}}\, \mathbf{n}^{pq} \otimes d\mathbf{n}^{pq}$	−4.5
$d\overline{\boldsymbol{\sigma}}^{\text{dn}^{\ell};\,\text{f}^{\text{t}}}$	$\frac{1}{V}\sum \quad f^{pq,\text{t}} \quad \ell^{pq,\text{n}}\, \mathbf{t}^{pq} \otimes d\mathbf{n}^{pq}$	0
$\sum = d\overline{\boldsymbol{\sigma}}$	$d(\frac{1}{V}\sum \mathbf{f}^{pq} \otimes \mathbf{l}^{pq})$	−0.6

[a] Sums $\sum$ are for the set of particle contacts $pq \in \mathcal{M}$.
[b] The deviator of each $(\cdot)$ contribution is the difference $d\overline{\sigma}_q^{(\cdot)} = d\overline{\sigma}_{22}^{(\cdot)} - d\overline{\sigma}_{11}^{(\cdot)}$.
[c] The rate of each $(\cdot)$ contribution is given in the dimensionless form $d\overline{\sigma}_q^{(\cdot)}/(-p_{\text{o}}\dot{\epsilon}_{22}\,dt)$.

The eight quantities on the right of (5) and (6) can be substituted into (2) to distinguish eight new contributions to the stress increment $d\overline{\boldsymbol{\sigma}}$, which we write as

$$
\begin{aligned}
d\overline{\boldsymbol{\sigma}} = d\overline{\boldsymbol{\sigma}}^{d\text{v}} + d\overline{\boldsymbol{\sigma}}^{d\text{f}^{\text{n}}} + d\overline{\boldsymbol{\sigma}}^{d\text{n}^{\text{f}}} + d\overline{\boldsymbol{\sigma}}^{d\text{f}^{\text{t}}} + d\overline{\boldsymbol{\sigma}}^{d\text{t}^{\text{f}}} \\
+ d\overline{\boldsymbol{\sigma}}^{d\ell^{\text{n}}} + d\overline{\boldsymbol{\sigma}}^{d\text{n}^{\ell}} + d\overline{\boldsymbol{\sigma}}^{d\ell^{\text{t}}} + d\overline{\boldsymbol{\sigma}}^{d\text{t}^{\ell}} \,.
\end{aligned}
\tag{7}
$$

The superscripts df^{n}, df^{t}, $d\ell^{\text{n}}$, and $d\ell^{\text{t}}$ denote the effects of changes in the scalar sizes of f^{n}, f^{t}, ℓ^{n}, and ℓ^{t}; whereas the superscripts dn^{f}, dt^{f}, dn^{ℓ}, and dt^{ℓ} denote the corresponding changes in the directions of $\mathbf{n}^{pq}$ and $\mathbf{t}^{pq}$ and their effects on $\mathbf{f}^{pq}$ and $\mathbf{l}^{pq}$. For the two-dimensional setting of circular disk particles, the final two terms in (7) are zero Although removing these two contributions simplifies (7), we will further expand (7) by separating the contributions of the normal and tangential components of forces $\mathbf{f}^{pq}$ within the two terms $d\overline{\boldsymbol{\sigma}}^{d\ell^{\text{n}}}$ and $d\overline{\boldsymbol{\sigma}}^{d\text{n}^{\ell}}$.

Our primary interest is in the contribution of each term in (7) to the deviator stress rate $d\overline{\sigma}_q = d\overline{\sigma}_{22} - d\overline{\sigma}_{11}$ at the peak state. The results are shown in Table 1, which itemizes nine contributions to the average deviator stress increment $d\overline{\boldsymbol{\sigma}}$ at the peak state. The values in the table are in a dimensionless form, as the various stress increments have been divided by the initial assembly mean stress $p_{\text{o}} = \frac{1}{2}(\overline{\sigma}_{11}+\overline{\sigma}_{22})$ at the start of the loading and by the compressive deformation increment $-\dot{\epsilon}_{22}\,dt$. In the last column of Table 1, positive rates correspond to a stiffening (hardening) of the material; negative values imply a softening effect. For the strain at which the results are taken—roughly at the peak state—the material had begun to soften, with a rate $d\overline{\sigma}_q/(-p_{\text{o}}\dot{\epsilon}_{22}\,dt)$ of −0.6. This slight softening is nearly zero, and is insignificant when compared with the initial assembly stiffness of 1760.

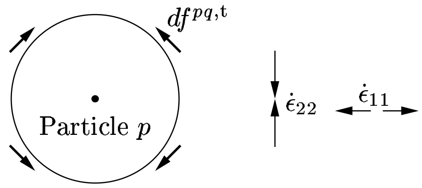

FIG. 2. Average directions of tangent force increments at the peak state. Neighboring particles move, on average, in the opposite directions.

At the peak state, the normal contact forces $f^{pq,\mathrm{n}}$ are increasing (becoming more compressive), and, by themselves, these changes would produce a stiffness of 14.0 (Table 1). This stiffness results from increases in the (compressive) normal contact forces among contacts that are preferentially aligned in the direction of the compressive strain $\dot{\epsilon}_{22}$. The hardening effect of the $df^{pq,\mathrm{n}}$ increments is primarily counteracted by two concurrent effects. Changes in the tangential forces $df^{pq,\mathrm{t}}$ produce a softening rate of -4.1. This trend is illustrated in Fig. 2, which shows the directions in which the tangential contact forces are changing (in the mean) at the peak state. Softening is also produced by the changes in the orientations of the contacts, as existing contacts tend to traverse the surfaces of particles in directions opposite those shown in Fig. 2 during the vertical compression. That is, neighboring particles q tend to rotate around a particle p in directions opposite those in Fig. 2, thus changing the contact normals $\mathbf{n}^{pq}$. These changes in direction produce the two equal softening rates of -4.5 in Table 1.

CONCLUSION

The microstructure of granular materials can evolve during loading even while the stress is stationary. To study the bulk behavior under these conditions, we must not only consider the effect of changing normal contact forces, but we must also include the usually incidental effects of the tangent forces and of the changes in contact orientations.

REFERENCES

Christoffersen, J., Mehrabadi, M. M., and Nemat-Nasser, S. (1981). “A micromechanical description of granular material behavior.” *J. Appl. Mech.*, ASME, 48(2), 339–344.

Kuhn, M. R. (2003). “Rates of stress in dense unbonded frictional materials during slow loading.” *Advances in Granular Materials: Fundamentals and Applications*, S. J. Antony, W. Hoyle, and Y. Ding, eds., Royal Society of Chemistry, London, U.K. In print.

Rothenburg, L. and Selvadurai, A. P. S. (1981). “A micromechanical definition of the cauchy stress tensor for particulate media.” *Mechanics of Structured Media, Part B*, A. P. S. Selvadurai, ed., Elsevier, Amsterdam, The Netherlands, 469–486.